Fabrication and Characterization of 2-dimensional Photonic Bandgap Crystal

C. I. Hsieh, H. L. Chen, W. C. Chao, and F. H. Ko, and S. C. Wu
National Nano Device Laboratories
1001-1 Ta Hsueh Road Hsinchu, Taiwan
R.O.C.

Abstract- In this paper, we demonstrate a simple and non-destructive measuring method for both TE and TM bandgaps of 2-dimensional (2D) silicon PBG by using reflected spectral ellipsometry. Although this measures the reflected light from samples, the transmitted signal of PBG layer can be measured by using reflecting signals. With large incident angles, planar PBG modulation effects and bandgap information can be obtained. To confirm this method, we fabricated silicon arrays for 2D PBG by using electron-beam lithography. From SEM pictures, we can verify the geometry especially the radius of the cells, which is related to the bandgaps. With a specific set of radii and dielectric constants, we can get the band diagram with plane-wave expansion method. There are several bandgaps of both TE and TM modes, and this sample can be used to detect multiple bandgaps.

Key-words: 2D photonic bandgap crystal, e-beam lithography, effective medium model, spectral ellipsometry

1 Introduction

Spatial refractive index modulation would lead light propagation into definitely different ways compared with bulk materials. Unlike random scattering, periodic structure would modulate light with specific rules. Light propagation in crystal have been generally used in various applications by its unique diffraction phenomena. Artificial periodic structures can be treated as crystal and used for visible and near infrared ray (NIR) applications. Such artificial crystal structures are called photonic crystal, or photonic bandgap (PBG) crystal [1].

The most important optical property of a PBG crystal is its bandgap behavior. In the bandgap region, there are no corresponding optical states and the light is highly reflective. A PBG crystal reflects perfectly in theory and can be designed as mirrors, guiding claddings, and other applications. The main difficulties of PBG crystals are their fabrication and characterization. The band structure becomes more obvious with smaller structure period to wavelength ratios (a / λ) that are also called eigenfrequencies of PBG structures, and the corresponding high reflection wavelength regime becomes broader. Small eigenfrequency needs sub-micron critical dimension (CD) structures, and semiconductor fabrication methods are suitable for PBG fabrication. Although semiconductor process can fabricate small CD structures, it is difficult to apply in 3-dimensions (3D) case. This is the reason the main PBG crystal structures are 2-dimensions (2D).

The other problem of PBG development is measurement. The common method in determining 2D PBG structure properties is by measuring the transmittance and reflection spectra from the PBG waveguide [2,3]. Coupling loss and out-of-plane loss highly decrease the PBG effects. In this work, out-of-plane propagation spectra are used to characterize optical band properties without coupling loss. The ellipsometer can determine the relationship

between theTE and TM through the 2D PBG layers. By canceling the effects of bulk substrates and thin-film effects, the PBG can be characterized.

2. Fabrication Setup

In the 2D PBG structures fabrication, traditional semiconductor process is suitable [4]. The state of the art process ability of semiconductor fabrication can fabricate structures with small critical dimension below 100 nm. Eigenfrequency range 0.3-0.5 can be fabricated with such process ability with designed working wavelength in the visible regime.

In addition to the 2D pattern definition, the PBG structure depths are also important in PBG applications. Enough structure depths can provide more electromagnetic fields involved with periodic structure modulations. In the ideal 2D PBG simulation, infinite structure depths are used to neglect the out of PBG structure plane losses. But large depth structures cannot easily fabricated by standard process and other fabrication methods such as micromechanical system fabrication and self-assembly process may need to be used. In this work, 0.5 μ m-depth structures are designed and fabricate so as to provide enough out-of-plane interactions. 550-nm thickness oxide layers are used as standard hard masks in etching process with sub-micro CD structures applications.

Fig. 1 shows the designed structure and the process flows. The hard masks are deposited 550-nm-thickness wet oxide on the silicon substrate by ASM furnace. Next step is to define photoresist patterns by an e-beam machine (Leica WEPRINT200). Negative tone photoresist (Sumitomo NEB22) of thickness 700 nm is used for pillar-like periodic structures. Table 1 shows the relationship between e-beam exposing doses and the fabricated PR patterns. The pattern is transferred to the oxide layer with oxide etcher (TEL S5000).The etch selectivity between oxide and resist is 1-1.5 for complete pattern transferring to the 550 nm oxide layer. The final PBG structure is composed of silicon pillars and transferred from the oxide pattern with poly-silicon etcher (LAM TCP 9400SE). In the silicon etching process, dip and perpendicular sidewalls are desired. The fabricated pillar widths are 116 nm and the period is 200 nm. After defining the silicon pattern, the resist and oxide are removed to obtain a pure silicon pattern without other material remaining as shown in Fig. 2.

Fig.3 shows the corresponding band diagram of the fabricated patterns [5]. Table 2 lists the band information from the band plot as shown in Fig.3.

3. Spectral ellipsometry for PBG structures

The ellipsometry measurement scheme for PBG is shown in Fig. 4. Ellipsometry parameters can be used to characterize PBG structures because of the relationship between different polarization states. By examining the ellipsometry parameters, PBG effects can be characterized. Ellipsometers measure $\tan(\psi)$ and $\cos(\delta)$. Ellipsometry parameters are defined as following forms [6],

$$\frac{\rho_{TM}}{\rho_{TE}} = \frac{E_{r,TM} / E_{i,TM}}{E_{r,TE} / E_{iTE}} = \tan(\Psi) e^{j\delta} \qquad (3)$$

where ρ_{TM} and ρ_{TE} are reflective coefficients of TM and TE polarized fields which are the ratio of reflected fields normalized with incident fields. Eq. (3) can be rewritten as the following form

$$\tan(\Psi) = \left| \frac{\rho_{TM}}{\rho_{TE}} \right|$$
$$\cos(\delta) = real\left(\frac{\rho_{TM} / \rho_{TE}}{\left| \rho_{TM} / \rho_{TE} \right|} \right) \qquad (4)$$

where $\tan(\psi)$ represents the reflection ratio and $\cos(\delta)$ represents the phase difference through the material-light interaction. For oblique incidence, TE and TM polarized light is reflected in different ways through PBG structures. As mentioned previously, the reflection happens within the band gap region. The reflection of different polarized light would manifest differently in their corresponding spectra. The reflection caused by TE bandgaps would appear as a dip in the $\tan(\psi)$ spectrum, while a TM reflection would lead a peak value of $\tan(\psi)$. Different polarized light through a medium also leads to different phase change, and $\cos(\delta)$ shows such changes. Effective film depths differ for polarization type and cause optical path differences which change $\cos(\delta)$ from the light source. Fig. 5 is the measured ellipsometry parameters along lattice direction Γ-X. In Fig. 5, the ellipses label the TE complete bandgaps

and the rectangles label the TM partial bandgaps along propagation lattice vectors. The TM complete bandgaps don't occur in this geometry from plane-wave calculation. TM partial bandgaps lead higher TM reflection and corresponding higher $\tan(\psi)$ values. Meanwhile, the TM polarized light would decrease its optical paths, leading to phase lags, and increase $\cos(\delta)$. On the other hand, TE bandgaps would decrease $\tan(\psi)$ and $\cos(\delta)$ values. The measured bandgaps from the spectrums of ellipsometry parameters are listed in Table 2. There are still other $\tan(\psi)$ and $\cos(\delta)$ changes without bandgap labels. This may have happened because of the constant and lossless refractive index assumption, and higher order bandgaps errors in the calculations. To solve the calculation problem, small period with lower order eigenfrequencies ranges should be adopted, and dispersion relation and loss properties of material should be introduced in the calculation. Furthermore, low index contrasts would lead to out-of plane loss into substrate and lower the ellipsometry signal. Higher confinement design should be used to improve the measurement.

4. Conclusion

Reflective spectral ellipsometry measurement can be applied in determining PBG effects by comparing ellipsometry spectra with calculated band diagrams. Theoretical calculation adopting the plane-wave expansion method can solve uniform PBG structures with high efficiency. With specific material and geometry, band diagram of different polarized light can be solved in the eigenfunction forms. Following the calculated parameters, 2D PBG crystal can be fabricated by traditional semiconductor process. By using e-beam lithography, submicron 2D PBG patterns can be defined.

The effective medium model can get the equivalent PBG film structure. To treat the 2D photonic crystal as films, the thin-film theory can calculate its corresponding film behavior. Refractive index differences provide confinement out-of-plane loss of 2D photonic crystal and provide non-infinite thick in the third direction of 2D structure originated from 2D assumption.

Ellipsometry parameter spectra excluding film behavior can be used to measure PBG signals. Since PBG provide state-free and high reflection in the bandgap region, the corresponding reflectance of different polarization can be observed in the $\tan(\psi)$ spectra. Moreover, the state-free regions decrease the optical path in the PBG structure and also change $\cos(\delta)$. By observing their ellipsometry parameters, we can measure the bandgap wavelengths of PBG without damage and complicated coupling issues.

References:

[1] E. Yablonovitch, "Inhibited spontaneous emission in solid-state physics and electronics", Phys. Rev. Lett. Vol. 58, 1987, pp. 2059-2062.

[2] Scherer, O. Painter, J. Vuckovic, M. Loncar, and T. Yoshie, "Photonic crystals for confining, guiding, and emitting light", IEEE Trans. Nanotech., Vol. 1, No. 1, 2002, pp. 4-11.

[3] J. S. Foresi, P. R. Villeneuve, J. Ferrera, E. R. Thoen, G. Steinmeyer, S. Fan, J. D. Joannopoulos, L. C. Kimerling, H. I. Smith, and E. P. Ippen, "Photonic-band microcavities in optical waveguides", Nature, Vol. 390, 1997, pp. 143-145

[4] Y. Chang, and S. M. Sze, "ULSI technology", McGRAW-Hill, 1996

[5] S. Guo and S. Albin, "A simple plane wave implementation method for photonic crystal calculations", Opt. Express Vol. 11, No. 2, 2003, pp.167-175.

[6] R. M. A. Azzam, and N. M. Bashara, "Ellipsometry and polarized light", North-Holland Physics publishing, 1977.

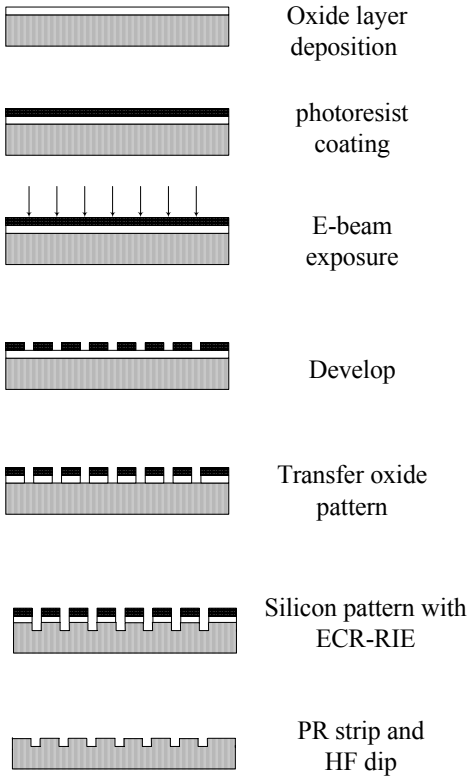

Fig. 1. 2D PBG structure process flow utilizing semiconductor process

No.	1	2	3	4	5
Dose ($\mu C/cm^2$)	8	10	12	14	17
CD (nm)	116	118	149	160	151

Table 1 Table of e-beam exposing doses and the corresponding critical dimensions (CD) of the fabricated patterns

No	gap mid	gap half width	polarization
1st	0.22	0.04	TE
2nd	0.39	0.05	TE
3rd	0.56	0.04	TE
1st	0.30	0.01	TM

Table 2 Comparison bandgap signal with calculated band diagram

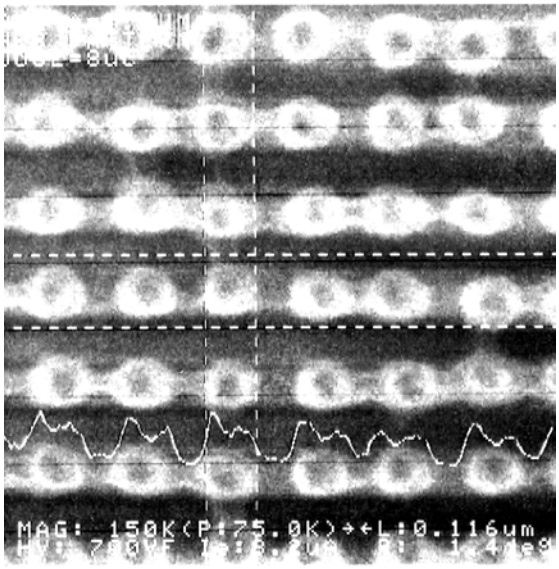

Fig. 2. SEM picture of fabricated 2D PBG structure

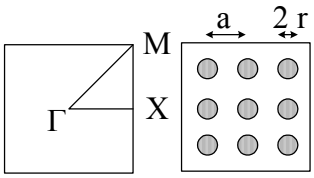

(a)

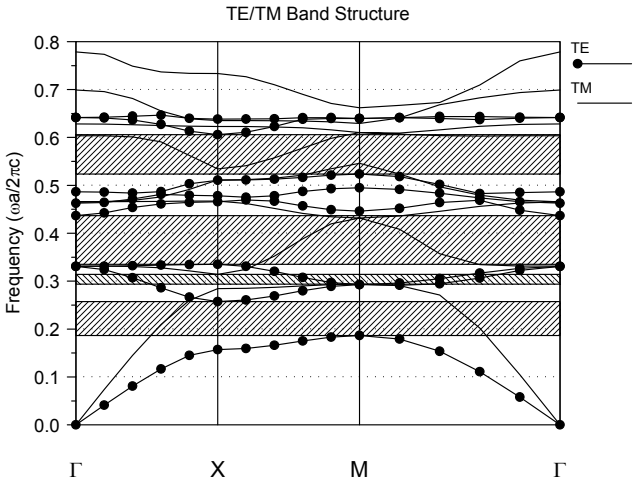

(b)

Fig. 3. (a) Schematic of rectangular PBG structure, and (b) the band diagram of designed PBG crystal.

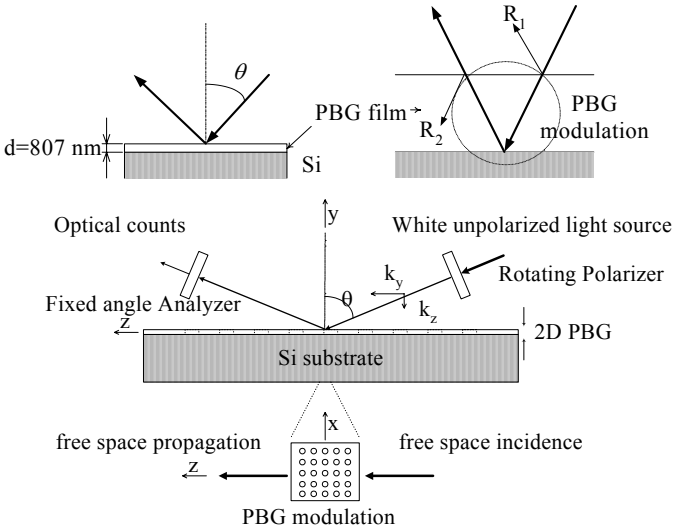

Fig. 4. Schematic of spectral ellipsometry measurement

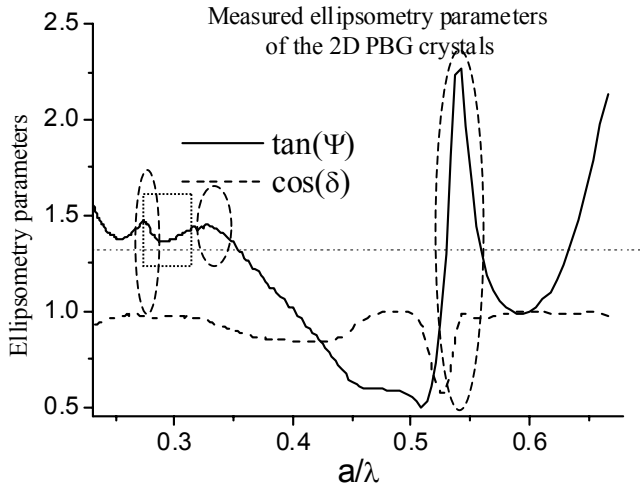

Fig. 5. Measured spectrum of PBG ellipsometry parameters